

Cu(II), Co(II), Ni(II), Mn(II) and Zn(II) Schiff base complexes of 3-hydroxy-4-[N-(2-hydroxynaphthylidene)-amino]-naphthalene-1-sulfonic acid: Synthesis, Spectroscopic, thermal, and antimicrobial studies

Safyah B. Bakare

Faculty of Education, Shaqra University, Al Muzahimiyah, Shaqra, Riyadh Province, P.O. Box 90, Zip Code 11921, Kingdom Saudi Arabia

Corresponding author: e-mail: safyahbakare@gmail.com

Five divalent transition metals Cu(II), Co(II), Ni(II), Mn(II) and Zn(II) complexes have been synthesized using 3-hydroxy-4-[N-(2-hydroxynaphthylidene)-amino]-naphthalene-1-sulfonic acid (H_3L) Schiff base as a ligand derived from the condensation reaction between 4-amino-3-hydroxynaphthalene-1-sulfonic acid and 2-hydroxy-1-naphthaldehyde. The synthesized complexes were characterized using microanalytical, conductivity, FTIR, electronic, magnetic, ESR, thermal, and SEM studies. The microanalytical values revealed that the metal-to-ligand stoichiometry is 1:1 with molecular formula $[M^{2+}(NaL)(H_2O)_x] \cdot nH_2O$ (where $x = 3$ for all metal ions except of Zn(II) equal $x = 1$; $n = 4, 10, 7, 4,$ and 6 for Cu(II), Co(II), Ni(II), Mn(II) and Zn(II), respectively). The molar conductivity result indicates that all these complexes are neutral in nature with non-electrolytic behavior. Dependently on the magnetic, electronic, and ESR spectral data, octahedral geometry is proposed for all the complexes except to zinc(II) complex is tetrahedral. Thermal assignments of the synthesized complexes indicates the coordinated and lattice water molecules are present in the complexes. SEM micrographs of the synthesized complexes have a different surface morphologies. The antimicrobial activity data show that metal complexes are more potent than the parent ligand.

Keywords: Schiff base; hydroxynaphthalene-1-sulfonic acid; hydroxy-1-naphthaldehyde; transition metal ions; morphology; antimicrobial activity.

INTRODUCTION

Schiff bases, as well as their complexes, are considered as a privileged class of compounds due to their catalytic activities, electrochemical analysis, anti-inflammatory, antiviral, anti-fungal, anti-malarial, as well as, biochemical synthesis^{1,2}. Schiff bases are of interest in industrial fields due to their corrosion inhibitor characters, thermostable materials, also, they considered powerful ligands for the formation of coordination complexes³. Schiff bases succeeded to occupy a vital position as ligands in coordination chemistry. Schiff's bases⁴ were still observed as one of the most potent groups of organic compounds in facile synthesis of metalloorganic hybrid compounds. Moreover, their interest in the synthesis of Schiff bases by condensation of 4-amino-3-hydroxy-1-naphthalene sulfonic acid with different aldehydes such as 5-bromosalicylaldehyde and 2-hydroxy-1-naphthaldehyde^{5,6} due to their potential applications in various fields. Noteworthy, the properties of Schiff bases stimulated much interest due to their contributions to material science, single molecule-based magnetism, and catalysis of many reactions such as reduction, oxidation, carbonization⁷, and release and binding of metal ions carried out with facilitated transport membranes. Schiff bases had been used in many industrial purposes such as polymer stabilizers, pigments, catalysts in some reactions such as polymerization reduction reaction of thionyl chloride to ketone, in addition, oxidation of organic intermediates⁸. Schiff's bases plays an important role in both the pharmaceutical, medical, and biological fields. They were, also, found to exhibit a broad range of biological activities, including antibacterial, antifungal, antiproliferative, antimalarial, and antipyretic properties⁹⁻¹².

According the above literature survey, I have decided to synthesis and discussed the structural characterization,

morphological, thermal and biological activity studies of the Cu(II), Co(II), Ni(II), Mn(II) and Zn(II) complexes with 3-hydroxy-4-[N-(2-hydroxynaphthylidene)-amino]-naphthalene-1-sulfonic acid (H_3L) Schiff base as ligand.

2-EXPERIMENTAL

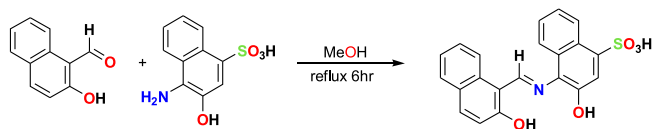
2-1-Reagents

The transition metal salts e.g. $CuCl_2 \cdot 2H_2O$, $CoCl_2 \cdot 6H_2O$, $NiCl_2 \cdot 6H_2O$, $MnCl_2 \cdot 4H_2O$, and $ZnCl_2$ were received from Sigma-Aldrich (Taufkirchen, Germany). The 4-amino-3-hydroxynaphthalene-1-sulfonic acid and 2-hydroxy-1-naphthaldehyde were purchased from Aldrich (Taufkirchen, Germany) chemical company. The distilled water, methanol, and diethyl ether solvents were used without distillation.

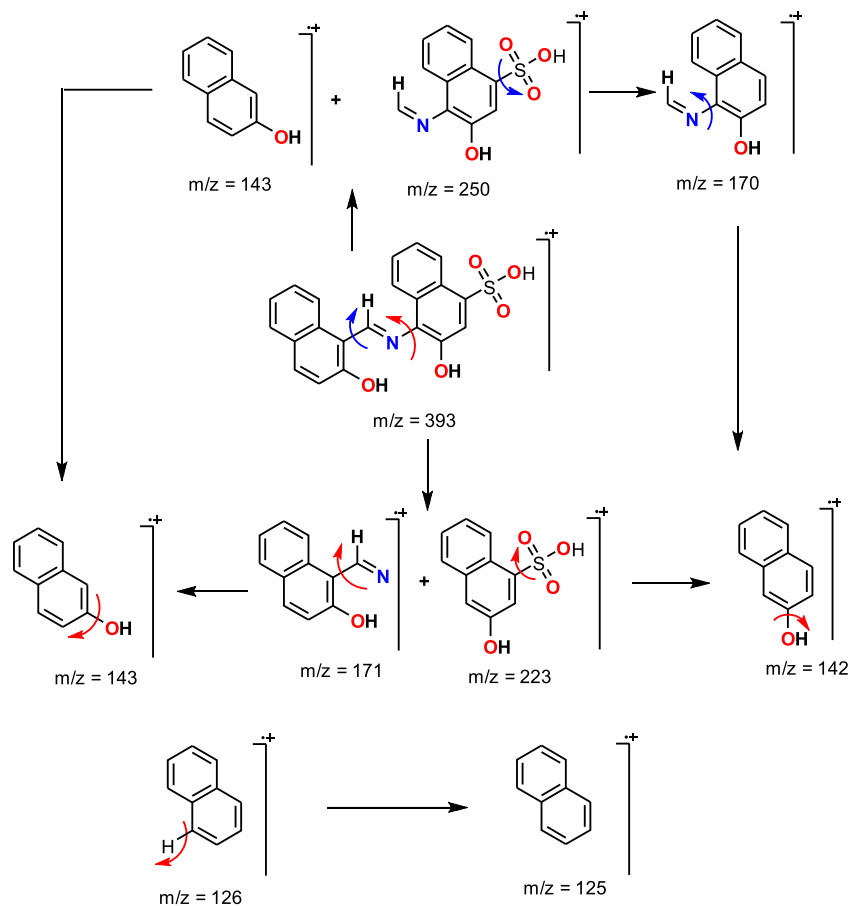
2-2-Synthesis of 3-hydroxy-4-[N-(2-hydroxynaphthylidene)-amino]-naphthalene-1-sulfonic acid (H_3L) Schiff base Schiff base

A mixture of 4-amino-3-hydroxynaphthalene-1-sulfonic acid (0.239 g, 1 mM) and 2-hydroxy-1-naphthaldehyde (0.172 g, 1 mM) in methanol (20 mL) was stirred under reflux for 6hr^{13,14}. An orange powder of HL was precipitated in good yield (Scheme 1). The orange powder was separated by filtration at room temperature and recrystallized from methanol. The purity of HL was insured by TLC. Yield, (91%), m.p 264–266°C. Anal. Calc. for $C_{21}H_{15}NO_5S$: C, 64.11; H, 3.84; N, 3.56; S, 8.15. Found: C, 63.91; H, 3.77; N, 3.43; S, 8.06%. ¹HNMR (300 MHz, DMSO d_6 , ppm) $\delta = 7.41-8.12$ (m, 11H, ArH), 7.90 (s, 1H, SO_3H), 9.70 (s, 1H, naphthyl-3-OH), 9.94 (s, 1H, CH=N), 12.00 (s, 1H, naphthyl-2-OH). ¹³CNMR (75 MHz, DMSO d_6 , ppm) $\delta = 107.5, 110.4, 120.9, 122.9, 123.6, 123.8, 125.2, 126.1, 126.9, 127.1, 127.4, 128.4, 128.8,$

136.2, 137.0, 137.8, 139.0, 142.9, 147.8, 162.7, and 166.0 ppm due to C=C, C=N, C-N, C-S and C-O). Mass spectra (Scheme 2), $[M^+]$ $m/z = [M^+ + 2]$ 395 (0.54%), $[M^+]$ 393.0 (43%), 250.6 (21.0), 171 (38.9%), 170 (60.4%), 143 (31.5%), 142 (29.8%), 126 (45.5%), 125 (22.8%).



Scheme 1. Synthesis of 3-hydroxy-4-[N-(2-hydroxynaphthylidene)-amino]-naphthalene-1-sulfonic acid (H_3L) Schiff base ligand



Scheme 2. Mass fragmentations of 3-hydroxy-4-[N-(2-hydroxynaphthylidene)-amino]-naphthalene-1-sulfonic acid (H_3L) Schiff base ligand

2-3-Synthesis of Cu(II), Co(II), Ni(II), Mn(II) and Zn(II) H_3L complexes

A hot methanolic solution of the respective metal chloride ($CuCl_2 \cdot 2H_2O$, $CoCl_2 \cdot 6H_2O$, $NiCl_2 \cdot 6H_2O$, $MnCl_2 \cdot 4H_2O$, and $ZnCl_2$) (1 mM) was added to the hot methanolic solution of ligand (H_3L) (1 mM). The pH of the mixtures were adjusted to the pH in the range of 7–8 with NaOH solution. The mixed solution was stirred at 70°C temperature for 1½ hr. The reaction mixture then concentrated to half its initial volume. The precipitates thus separated out, were washed with methanol and dried in *vacuo*.

2-4-Instrumental analyses

The percentage of %C, %H and %N elements were determined using Perkin-Elmer CHN 2400 analyzer. Percentage of metal ions was estimated gravimetrically. Molar conductivities were scanned using Jenway 4010

using AEI MS 30 mass spectrometer at 70 eV. Scanning electron microscopy model was Joel JSM-6390LA with an accelerating voltage of 20 KV.

2-5-Antimicrobial assessments

Antibacterial inhibition were tested by using diffusion method¹⁵, this biological experiment was performed three times to take total average data. The ciprofloxacin pure drug was used as antibacterial standard. The tested samples were assessed at 10 and 50 mg concentrations. The antibacterial activity of free HL ligand and their complexes were applied against:

conductivity meter. Magnetic measurements were calculated using magnetic balance (Sherwood Scientific), Cambridge, England. Infrared spectra were recorded in KBr discs using a Bruker FT-IR Spectrophotometer within 4000–400 cm^{-1} range. Electronic spectra of the synthesized Schiff base and its complexes with concentration of 1.0×10^{-3} mol/ cm^3 were scanned using Perkin-Elmer Precisely Lambda 25 UV/Vis double beam Spectrometer fitted with a quartz cell of 1.0 cm path length. ¹H-NMR spectra of Schiff base in DMSO solutions were scanned using 200 MHz Varian Gemini Spectrophotometers using TMS as the internal standard. Thermal analyses were performed using a Shimadzu thermo gravimetric analyzer under N_2 at 800°C was used for recording thermal measurements (TG/DTG–50H) using a single loose top loading platinum sample pan under nitrogen atmosphere at 30 ml/min flow rate and a 10°C/min heating rate in the temperature range 25–800°C. Mass spectra were scanned

Gram positive bacteria: *Bacillus Subtillus* (RCMB 00010) and *Staphylococcus aureas* (RCMB 000106). Gram negative bacteria: *Escherichia Coli* (RCMB 000103) and *Pseudomonas aeruginose* (RCMB 000102).

A 100 μL of the tested samples which dissolved in dimethylsulfoxide with different concentrations 10 mg/mL and 50 mg/mL were assessed against two kinds of fungi (*A. Niger* and *Penicillium sp.*). The free sample of DMSO was used as control and also fluconazole drug was used as antifungal standard.

RESULTS AND DISCUSSION

3-1-Microanalyses and physical properties

The microanalytical result and physical properties of the H_3L ligand and its Cu(II), Co(II), Ni(II), Mn(II) and Zn(II) complexes are summarized in Table 1. The Schiff base ligand (H_3L) is soluble in common organic solvents. The synthesized Schiff base complexes are insoluble in alcohols, benzene, and nonpolar solvents (CHCl_3 , CH_2Cl_2 , and CCl_4) but soluble in DMSO and DMF with gently heating. The elementary analyses data indicate that the metal-to-ligand ratio is 1:1 in all the synthesized complexes. The conductivity data of all the metal complexes indicates that all are non-electrolyte nature within 2.50–4.43 μS range¹⁶.

Table 1. Analytical and physical properties of H_3L Schiff base and its complexes

Molecular formula	Color	Λ_m [μS]	Elemental analyses, Found/[Calcd.%]				Mp, $^\circ\text{C}$
			C	H	N	M	
H_3L	Orange	1.20	64.08 (64.11)	3.54 (3.84)	3.29 (3.56)	–	264
$[\text{Cu}(\text{NaL})(\text{H}_2\text{O})_3] \cdot 4\text{H}_2\text{O}$ (I)	Brown	3.33	41.22 (41.83)	4.19 (4.35)	2.20 (2.32)	10.43 (10.54)	> 300
$[\text{Co}(\text{NaL})(\text{H}_2\text{O})_3] \cdot 10\text{H}_2\text{O}$ (II)	Dark brown	2.50	35.55 (35.70)	5.30 (5.42)	1.86 (1.98)	7.99 (8.34)	> 300
$[\text{Ni}(\text{NaL})(\text{H}_2\text{O})_3] \cdot 7\text{H}_2\text{O}$ (III)	Deep green	4.43	38.54 (38.67)	4.76 (4.95)	1.98 (2.15)	8.87 (9.00)	> 300
$[\text{Mn}(\text{NaL})(\text{H}_2\text{O})_3] \cdot 4\text{H}_2\text{O}$ (IV)	Brown	4.12	41.99 (42.43)	4.33 (4.41)	2.11 (2.36)	9.15 (9.24)	> 300
$[\text{Zn}(\text{NaL})(\text{H}_2\text{O})] \cdot 6\text{H}_2\text{O}$ (V)	Light brown	2.98	41.55 (41.70)	4.21 (4.33)	2.24 (2.32)	10.77 (10.81)	> 300

3-2-Infrared spectra

Infrared spectral data of the H_3L Schiff base ligand and its metal complexes are displayed in (Fig. 1) and their assignments are listed in Table 2. The infrared spectrum of ligand (H_3L)⁶ has a distinguish band at 1618 cm^{-1} , assignable to the $\nu(\text{C}=\text{N})$ of azomethane group, showed a disappeared or shift to 27–74 cm^{-1} to a lower wavenumber in its complexes, indicating the participation of nitrogen of the azomethane group in coordination to the metal ion^{6, 17}. Regarding H_3L free ligand, the stretching vibration of $\nu(\text{O}-\text{H})$ band is disappeared after complexation due to the deprotonation –OH groups and coordinated oxygen atom towards central metal ions. The $\nu(\text{C}-\text{O})$ stretching vibration of phenolic group display at 1270 cm^{-1} in case of H_3L Schiff base ligand, this band is shifted to lower wavenumbers after complexation because of involvement of phenolic group oxygen atom in the coordination by associated C–O–M bond¹⁸. In the free H_3L ligand the asymmetric vibrations of SO_3 group of sulfonic acid salt occur in the FTIR 1198 cm^{-1} range¹⁸. The band due to the symmetric stretching vibration is

sharper and occurs at 1079 cm^{-1} . The symmetric deformation modes of SO_3 group give medium weak bands at 614 and 551 cm^{-1} region¹⁹. The sulfonic group does not affect the conjugated system irrespective of the substitution position in the naphthalene rings. Changes in the electron density are relatively low at the carbon atoms to which sulfonic group are substituted²⁰. The participation of sulfur d-orbitals in the conjugated system is very low, and the π contribution into C–S bond is practically negligible²¹. The asymmetric stretching mode of SO_3 is mixed with C–N stretching, C–H in-plane bending²¹ giving a medium strong band at 1198 cm^{-1} in the IR spectrum. The observed band at 1079 cm^{-1} in the IR can be assigned to symmetric stretching vibrations of SO_3 group, vibrations that are mixed with naphthalene ring deformations²². The SO_3 symmetric bending vibrations are coupled with out-of-plane bending vibrations or with naphthalene ring deformations giving a medium weak bands at 614 and 551 cm^{-1} in the IR. The medium intense IR bands at 508 cm^{-1} and weak bands at 445 cm^{-1} correspond to SO_3 wagging vibrations. All the metal complexes showed a broad band in the range of 3450–3470 cm^{-1} , followed by another bands at 1693–1636 cm^{-1} and 800–900 cm^{-1} that suggests the presence of water molecules in the metal complexes²³. The involvement of oxygen and nitrogen atoms in coordination is confirmed by presence of new bands in the

bands at 33333 and 24570 cm^{-1} due to $\pi \rightarrow \pi^*$ and $n \rightarrow \pi^*$ of aromatic rings and azomethine group, respectively²⁴.

Table 2. Infrared spectra assignments of H_3L Schiff base and its metal complexes

Compounds	$\nu(\text{OH})$	$\nu(\text{C}=\text{N})$	$\nu(\text{M}-\text{N})$	$\nu(\text{M}-\text{O})$
H_3L	–	1618	–	–
I	3460	1591	606	488, 449
II	3470	1544	598	486, 448
III	3470	–	598	467, 445
IV	3451	1589	607	514, 447
V	3470	1553	598	467, 443

range of 607–597 cm^{-1} and 514–448 cm^{-1} corresponding to $\nu(\text{M}-\text{N})$ and $\nu(\text{M}-\text{O})$, respectively.

3-3-Electronic spectral studies

The electronic spectra of the free H_3L Schiff base chelate and its Cu(II), Co(II), Ni(II), Mn(II), and Zn(II) were performed using DMSO solvent. The electronic spectrum of free H_3L ligand has two essential absorption

The electronic spectrum of octahedral copper(II) complex contain two transition bands at 16950 cm^{-1} and 22222 cm^{-1} due to ${}^2E_g \rightarrow {}^2T_{2g}$ and ${}^2B_{1g} \rightarrow {}^2A_{1g}$ electronic transitions, respectively. Cobalt(II) complex UV-Vis spectrum has two transition bands at 19231 and 23809 cm^{-1} , these are assigned to electronic transition ${}^4T_{1g}(\text{F}) \rightarrow {}^4A_{2g}(\text{F})\nu_2$ and ${}^4T_{1g}(\text{F}) \rightarrow {}^4T_{1g}(\text{P})\nu_3$ of octahedral geometrical structural, respectively²⁴. Electronic transition spectrum of nickel(II) complex has three characteristic bands at 17241 , 20833 and 26316 cm^{-1} for the ${}^3A_{2g} \rightarrow {}^3T_{2g}(\text{F})$, (ν_1); ${}^3A_{2g} \rightarrow {}^3T_{1g}(\text{F})$, (ν_2) and ${}^3A_{2g} \rightarrow {}^3T_{2g}(\text{P})$, (ν_3) transitions of octahedral geometrical structure, respectively. The manganese(II) complex show two electronic bands at 18182 and 20000 cm^{-1} and other weak band at 24096 cm^{-1} for octahedral geometry. The absorption spectrum of zinc(II) complex has a three electronic transition bands at 35088 , 25316 and 21505 cm^{-1} due to intr-ligand charge transfer and $L-M_{CT}$ ²⁵.

3-4- Magnetic measurements

The practical magnetic moments of copper, cobalt, nickel, and manganese(II) complexes are 1.87, 4.85, 3.50, and 5.43 BM, these values are agreement with the characteristic of mononuclear octahedral geometry, respectively²⁶⁻²⁹. The observed magnetic moment value for the zinc(II) complex is zero, indicating diamagnetic nature of the complex.

3-5- Electron spin resonance assignments

The ESR spectrum of copper(II) complex (Fig. 1) was scanned at room temperature in the solid state. The spectrum show one intense absorption in the high field and is isotropic due to tumbling of the molecule. The g values of the complex are g_{\parallel} (2.1303) $>$ g_{\perp} (2.0157) $>$ 2.0023, indicating that the unpaired electron in the ground state of copper(II) ion is predominantly in $d_{x^2-y^2}$. The value of exchange interaction term G , estimated from the following equation is 9.55.

$$G = (g_{\parallel} - 2.0023)/(g_{\perp} - 2.0023)$$

If $G > 4.0$, the local tetragonal axes are aligned parallel or only slightly misaligned. If $G < 4.0$, significant exchange coupling is present and misalignment is appreciable. The observed value for the exchange interaction term "G" suggests that the complex has regular octahedral geometry^{30, 31}.

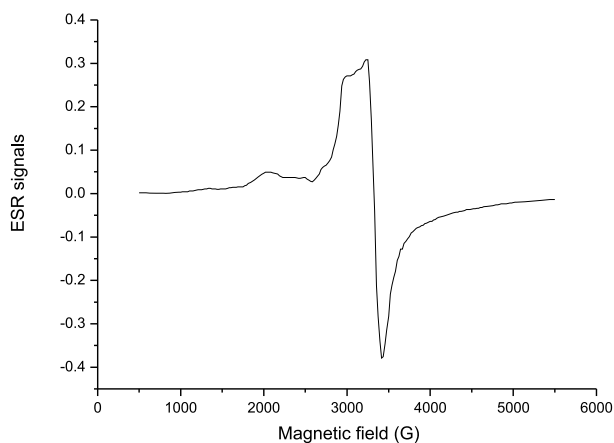


Figure 1. ESR spectrum of copper(II) complex

3-6- ${}^1\text{H}$ NMR spectra

The ${}^1\text{H}$ NMR spectrum of the H_3L Schiff base ligand is recorded in $\text{DMSO-}d_6$. In the ${}^1\text{H}$ NMR spectra of Schiff base ligand a peak at $\delta = 7.90$ ppm is assigned for the proton of SO_3H of Schiff base, singlet peaks at 9.70 and 12.00 ppm are attributed to 1H of naphthyl-3-OH group and a singlet at $\delta = 9.94$ ppm assignable for proton of azomethine group. The zinc(II) complex showed ${}^1\text{H}$ NMR (Fig. 2S) $\delta = 7.48$ – 8.18 (m, 11H, ArH), 8.88 (s, 1H, CH=N). This spectrum referred to upfield shift for the proton of azomethine group due to the change in electronic environment of the ligand in case of bonding with zinc metal ion. The disappearance of the proton of $-\text{OH}$ group confirmed that the chelation of the zinc(II) is carried out with oxygen of the $-\text{OH}$ group, also, the SO_3H proton is absent due to associated of sodium salt.

3-7- Thermal analysis

Figures 2 and 3S are referred to the TGA/DrTGA and DTA thermograms of H_3L Schiff base and its complexes Cu, Co, Ni, Mn and Zn(II) under nitrogen atmosphere at heating rate $10^\circ\text{C}/\text{min}$. The H_3L Schiff base ligand is decomposed in three DTA_{max} peaks at 274°C (endothermic), 403°C (endothermic), and 594°C (exothermic) within temperature range 25 – 800°C , respectively. The experimental total mass loss is 100%, this supported the purity of synthesized H_3L Schiff base ligand. The thermal decomposition of the Cu(II) complex occurs at three stages of $\text{DTA}_{\text{max}} = 75^\circ\text{C}$ (exo), 240°C (exo), and 460°C (endo) with found mass losses 77%, due to losses of L Schiff base ligand, four uncoordinated H_2O molecules, and three coordinated H_2O molecules. The final decomposition residue at 800°C is mixture from CuO and $\frac{1}{2}\text{Na}_2\text{O}$ oxides that agreement with the theoretical data. The Co(II) complex destroyed thermally in five steps at $\text{DTA}_{\text{max}} = 75^\circ\text{C}$ (exo), 132°C (exo), 260°C (exo), 370°C (exo), and 650°C (endo), respectively, corresponding to the loss of L Schiff base ligand, and thirteen of coordinated and uncoordinated water molecules. The total weight loss of the cobalt(II) complex is 84.80% and the percentage of residual is 15.20%. The CoO and $\frac{1}{2}\text{Na}_2\text{O}$ oxides associated after the thermal decomposition of cobalt(II) complex at 800°C . The thermal decomposition of Ni(II) complex pass through three maximum DTA decomposition steps at 83°C (exo), 233°C (exo), and 530°C (endo), respectively. The mass loss associated as 60.57% attributed to the loss of L Schiff base ligand, and ten of coordinated and uncoordinated water molecules. The final residue are nickel(II) oxide, sodium oxide that polluted with residual carbon atoms. The thermal decomposition of manganese(II) complex pass through four maximum DTA decomposition steps at 100°C (endo), 505°C (exo), 694°C (exo) and 725°C (exo), respectively. The mass loss associated as 48.50% attributed to the loss of L Schiff base ligand, and seven of coordinated and uncoordinated water molecules. The final residue are MnO_2 , sodium oxide that polluted with residual carbon atoms. Thermal decomposition of Zn(II) complex take place in definite four differential thermal peaks $\text{DTA}_{\text{max}} = 87^\circ\text{C}$ (exo), 273°C (exo), 330°C (endo) and 503°C (endo). The degradation stages occurs at a temperature ranges 25 – 800°C . The found weight loss

associated with these steps is 85.80% assigned to the loss of $7\text{H}_2\text{O}$ (coordinated and uncoordinated) and L Schiff base ligand species. Final thermal product at 800°C is ZnO and $\frac{1}{2}\text{Na}_2\text{O}$ oxides.

The results of the mentioned investigations (microanalytical, conductivity, FTIR, electronic, magnetic, ESR, TGA/DTA) support the suggested structure of the metal complexes. Cu(II) , Co(II) , Ni(II) , Mn(II) , and Zn(II) metal ions are forming 1:1 (M:L) complexes. Accordingly on elemental, conductance and spectral studies, six-coordinated geometry was assigned for Cu(II) , Co(II) , Ni(II) , and Mn(II) complexes. Based on the above results, the proposed structures of all the metal complexes have been shown in Fig. 3.

3-8- Kinetic thermodynamic parameters

Table 3 refer to the thermodynamic parameters (activation energy “ E^* ”, enthalpy of activation “ H^* ”, entropy of activation “ S^* ” and free energy of activation “ G^* ” of H_3L Schiff base complexes of copper(II), cobalt(II), nickel(II), manganese(II), and zinc(II) metal ions were calculated based on the TGA/DTA graphs. Accordingly of Coats–Redfern and Horowitz–Metzger^{32,33} relationships were used to estimated these parameters. The high values of $E^* = 76.5\text{--}202 \text{ KJ mol}^{-1}$ are assigned to the slower reactions of copper, cobalt, nickel, manganese and zinc(II) Schiff base complexes than normal³⁴. The $-ve$ values of ΔS^* ($-21.6\text{--}132 \text{ J mol}^{-1} \text{ K}^{-1}$) deduced that the activated solid complexes has a more ordered³⁵ than the parent reactants.

The surface morphology and grain size of the H_3L Schiff base and its cobalt(II) and nickel(II) complexes have

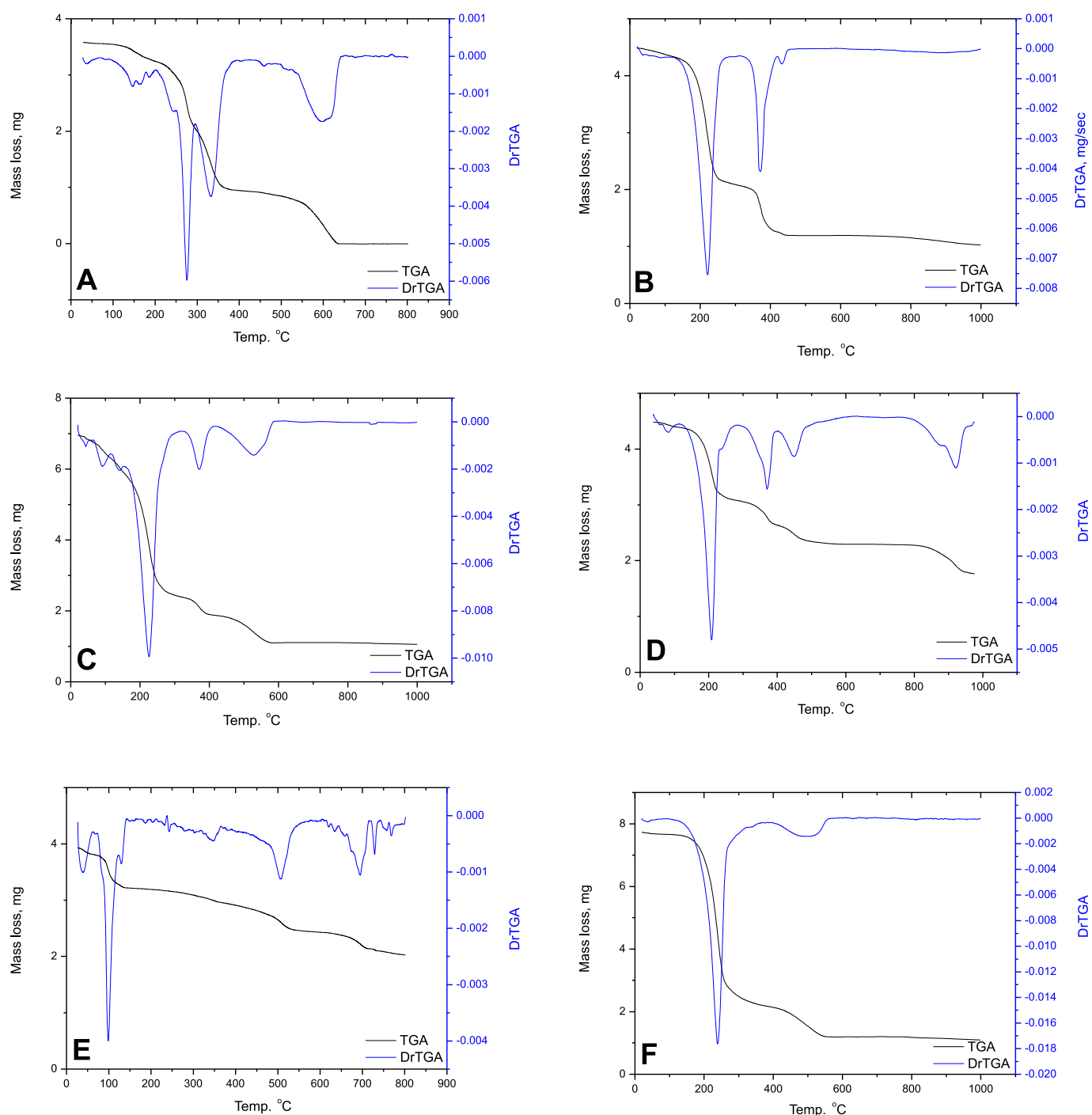


Figure 2. TGA/DrTGA curves of A: H_3L Schiff base and its complexes (B: Cu^{2+} ; C: Co^{2+} ; D: Ni^{2+} ; E: Mn^{2+} ; and F: Zn^{2+})

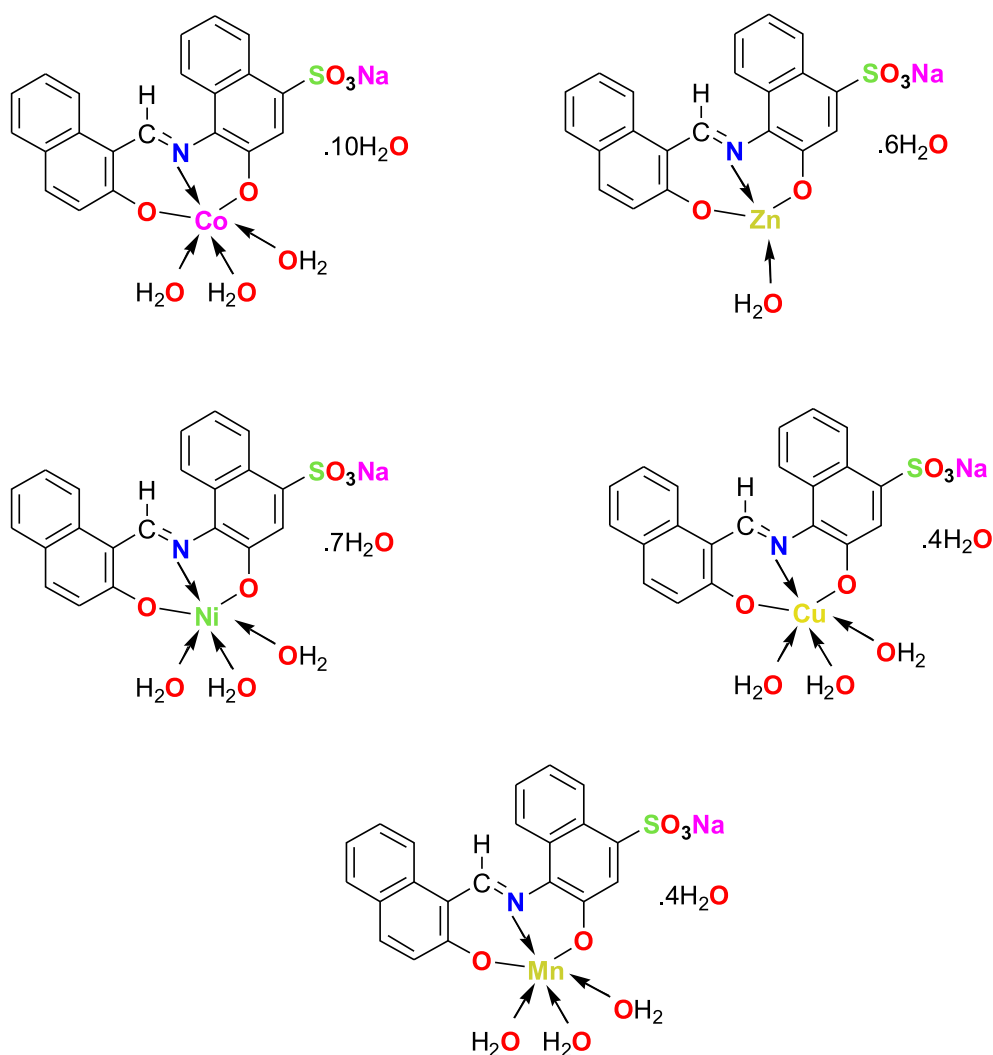


Figure 3. Suggested structures of Cu^{2+} ; Co^{2+} ; Ni^{2+} ; Mn^{2+} and Zn^{2+} Schiff base complexes

Table 3. Thermodynamic parameters of free H_3L Schiff base ligand and its complexes

Compound	Stage	Method*	Parameter				r
			E^* [J mol^{-1}]	ΔS^* [$\text{J mol}^{-1} \text{K}^{-1}$]	ΔH^* [J mol^{-1}]	ΔG^* [J mol^{-1}]	
H_3L	1 st	CR	7.93×10^4	-1.21×10^2	7.71×10^4	1.98×10^5	0.9921
		HM	8.43×10^4	-1.19×10^2	8.21×10^4	1.32×10^5	0.9911
I	2 nd	CR	1.11×10^5	-5.31×10^1	1.21×10^5	1.45×10^5	0.9985
		HM	1.12×10^5	-3.91×10^1	2.01×10^5	1.21×10^5	0.9911
II	3 rd	CR	0.90×10^5	-4.54×10^1	1.32×10^5	1.43×10^5	0.9984
		HM	1.01×10^5	-4.02×10^1	1.71×10^5	1.11×10^5	0.9932
III	2 nd	CR	7.65×10^4	-1.32×10^2	5.64×10^4	1.62×10^5	0.9912
		HM	8.19×10^4	-1.13×10^2	6.21×10^4	1.23×10^5	0.9972
IV	2 nd	CR	1.01×10^5	-4.32×10^1	2.11×10^5	1.23×10^5	0.9912
		HM	0.89×10^5	-3.65×10^1	1.92×10^5	1.11×10^5	0.9901
V	2 nd	CR	2.02×10^5	-4.32×10^1	2.31×10^5	1.43×10^5	0.9911
		HM	1.88×10^5	-2.16×10^1	2.17×10^5	1.22×10^5	0.9908

*Coats–Redfern (CR) and Horowitz–Metzger (HM)

been investigated by the scanning electron micrograph “SEM”. The SEM micrographs of the H_3L Schiff base and both $\text{Co}(\text{II})$ and $\text{Ni}(\text{II})$ complexes are shown in Fig. 4a-c. Regarding H_3L Schiff base and both $\text{Co}(\text{II})$ and $\text{Ni}(\text{II})$ complexes the SEM micrographs were taken in the scale range of 2–5 μm . From the SEM micrographs it was noted that there is a uniform matrix in case of H_3L Schiff base and both $\text{Co}(\text{II})$ and $\text{Ni}(\text{II})$ complexes. The micrograph of H_3L Schiff base shows round shaped balls like morphology, the cobalt(II) complex shows spongy forms and the Ni(II) complex shows long sticks like morphology.

3-10-Biological assay

Biological activity of the Schiff base ligand and its metal complexes were studied and results shows that the activity of the metal complexes is higher than the free Schiff base ligand. The antimicrobial activity of the H_3L Schiff base ligand and its copper(II), cobalt(II), nickel(II), manganese(II), and zinc(II) metal complexes were scanned against the four kind of bacteria (*Bacillus subtilis*, *Staphylococcus aureas*, *E. coli*, *Pseudomonas sp.*) and two fungi *Aspergillus Nigaer* and *Penicillium Sp.* by the diffusion method with well disc¹⁵. The samples were prepared in DMSO at a concentration of 10 and

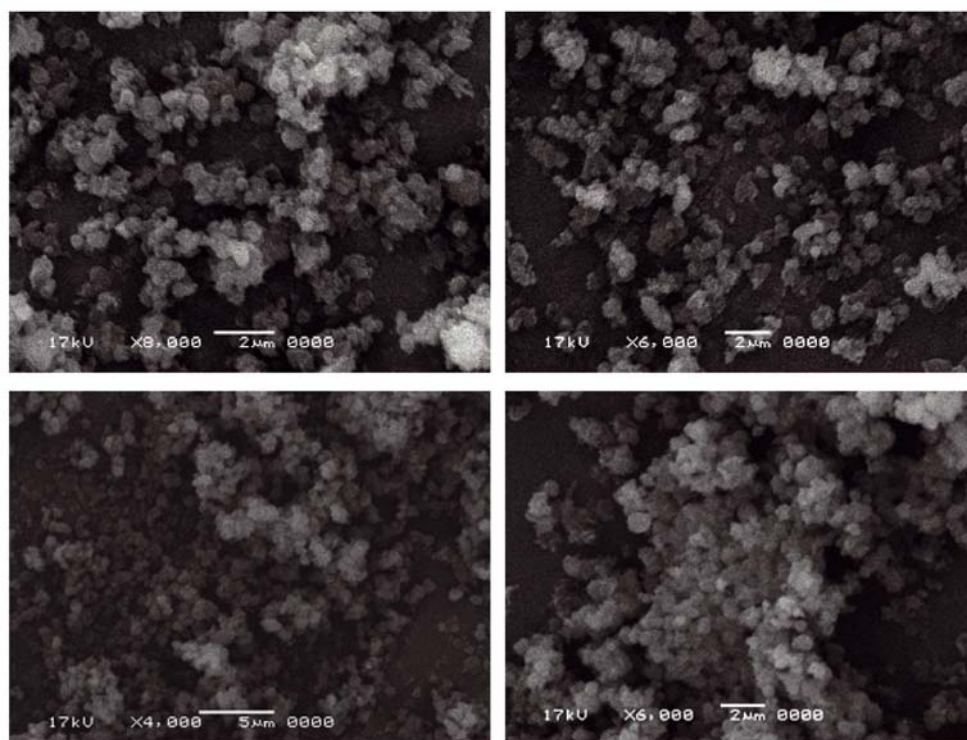


Figure 4a. SEM micrographs of H_3L Schiff base ligand with different magnifications within 2–5 μm scale

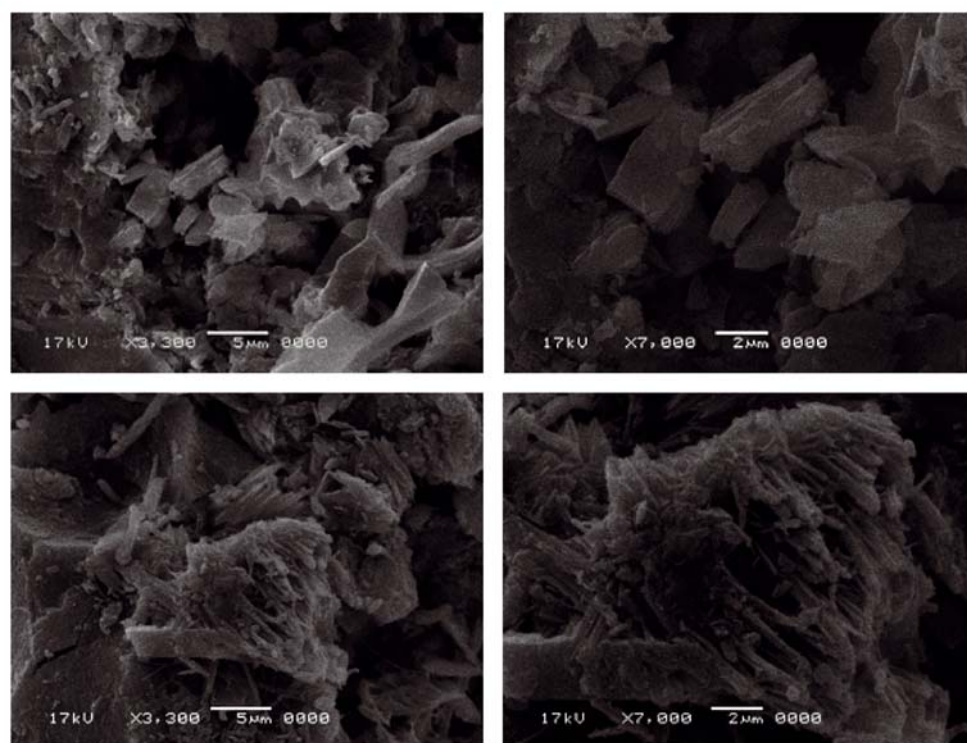


Figure 4b. SEM micrographs of $[Co(NaL)(H_2O)_3] \cdot 10H_2O$ complex with different magnifications within 2–5 μm scale

50 mg/mL. The inhibition zone were calculated by millimeter at 37°C after 24 hrs incubation. The antibacterial assessments are summarized in Table 4. The significant data in this table reveal to the activity of the Schiff base ligand after complexity with the metal ions became more pronounced. The presence of azomethine group and chelation effect with metal ions enhanced the antibacterial activities. Among all the complexes, the manganese(II) complex shows significant activity against bacteria and fungi. This enhancement activity of these synthesized metal complexes may be assigned

based on the chelation theory^{36–38}. After chelation, the polarity will be reduced to a greater extent due to the overlap of ligand orbital and the partial sharing of the positive charge of the metal ion with donor groups^{37, 38}. Moreover, the chelation process increases the delocalization of the π -electrons over the whole chelate ring, which results in an increase in the lipophilicity of the metal complexes³⁶. So, the metal complexes can easily penetrate into the lipid membranes and block the metal binding sites of enzymes of the microorganisms³⁸. These metal complexes also affect the respiration process of



Figure 4c. SEM micrographs of $[\text{Ni}(\text{NaL})(\text{H}_2\text{O})_3]\cdot 7\text{H}_2\text{O}$ complex with different magnifications within 2–5 μm scale

Table 4. Antibacterial activities of H_3L Schiff base ligand and its metal complexes at 10 and 50 mg concentrations

Sample	Gram Positive Bacteria				Gram Negative Bacteria				Antifungal Activity			
	<i>Bacillus subtilis</i>		<i>Staphylococcus aureus</i>		<i>E. coli</i>		<i>Pseudomonas sp.</i>		<i>Aspergillus Nigraer</i>		<i>Penicillium Sp.</i>	
	10 mg	50 mg	10 mg	50 mg	10 mg	50 mg	10 mg	50 mg	10 mg	50 mg	10 mg	50 mg
H_3L	–	3	–	1	3	2	1	6	–	2	–	–
$\text{Cu}(\text{II})$	8	19	2	21	3	15	12	18	9	16	14	20
$\text{Co}(\text{II})$	1	11	–	10	–	5	–	8	1	5	1	8
$\text{Ni}(\text{II})$	3	20	4	18	1	10	7	14	5	12	11	19
$\text{Mn}(\text{II})$	6	22	8	20	5	17	13	20	9	18	15	26
$\text{Zn}(\text{II})$	5	16	–	13	–	3	1	9	3	8	5	16
Ciprofloxacin	11	25	9	23	15	19	13	20	–	–	–	–
Fluconazole	–	–	–	–	–	–	–	–	10	21	16	28

the cell and thus block the synthesis of proteins, which restrict further growth of the organism³⁶.

CONCLUSION

A series of Schiff bases derived from 3-hydroxy-4-[N-(2-hydroxynaphthylidene)-amino]-naphthalene-1-sulfonic acid and their metal complexes (Cu, Co, Ni, Mn and Zn(II)) which were characterized by elemental analysis, Mass, ^1H NMR, ^{13}C NMR, FT-IR and UV-Vis spectral studies. Molar ratio of prepared complexes were 1:1 of (metal: ligand). The complexes which have the general formula $[\text{M}^{2+}(\text{NaL})(\text{H}_2\text{O})_x]\cdot n\text{H}_2\text{O}$ ($x = 3$ for all metal ions except of Zn(II) equal $x = 1$; $n = 4$ –10). The biological activity assay revealed that the synthesized Schiff base metal complexes have an antimicrobial efficiency rather than the starting materials.

LITERATURE CITED

- Al Zoubi, W. & Al Mohanna, N. (2014). Membrane sensors based on Schiff bases as chelating ionophores—A review. *Spectrochim. Acta, Part A*, 132, 854–870. doi.org/10.1016/j.saa.2014.04.176.
- Al Zoubi, W., Al-Hamdani, A.A.S. & Kaseem, M. (2016). Synthesis and antioxidant activities of Schiff bases and their complexes: a review. *Appl. Organomet. Chem.*, 30, 810–817. doi.org/10.1002/aoc.3506.
- Al Zoubi, W. & Ko, Y.G. (2017). Schiff base complexes and their versatile applications as catalysts in oxidation of organic compounds: part I. *Appl. Organomet. Chem.*, 31, e3574.
- Al-Hamdani, A.A.S., Balkhi, A.M., Falah, A. & Shaker, S.A. (2016). Synthesis and investigation of thermal properties of vanadyl complexes with azo-containing Schiff-base dyes. *J. Saudi, Chem. Soc.*, 20, 487–501.
- Duffy, K.J., Darcy, M.G., Delorme, E., Dillon, S.B., Eppley, D.F., Erickson-Miller, C., Giampa, L., Hopson, C.B., Huang, Y., Keenan, R.M., Lamb, P., Leong, L., Liu, N., Miller, S.G., Price, A.T., Rosen, J., Shah, R., Shaw, T.N., Smith, H., Stark, K.C., Tian, S.-S., Tyree, C., Wiggall, K.J., Zhang, L. & Luengo, J.I. (2001). Hydrazinonaphthalene and azonaphthalene thrombopoietin mimics are nonpeptidyl promoters of megakaryocytopoiesis. *J. Med. Chem.*, 44(22), 3730–3745.
- Shweta, Neeraj, Asthana, S.K., Mishra, R.K. & Upadhyay, K.K. (2016). Design-specific mechanistic regulation of the sensing phenomena of two Schiff bases towards Al^3 . *RSC Adv.*, 6, 55430–55437.
- Bose, D., Banerjee, J., Rahaman, S.K.H., Mostafa, G., Fun, H.K., Bailey, W.R.D., Zaworotko, M.J. & Ghosh, B.K. (2004). Polymeric end-to-end bridged cadmium(II)thiocyanates containing monodentate and bidentate N-donor organic

blockers: supramolecular synthons based on π - π and/or C-H... π interactions. *Polyhedron*, 23, 2045–2053.

8. El-Boraey, H.A. (2005). Structural and thermal studies of some aroylhydrazone Schiff's bases-transition metal complexes. *J. Therm. Anal. Calorim.*, 81(2), 339–346.

9. Al-Shirif, A.S.M. & Abdel-Fattah, H.M. (2003). Thermogravimetric and spectroscopic characterization of trivalent lanthanide chelates with some Schiff bases. *J. Therm. Anal. Calorim.*, 71, 643–649.

10. Grivani, G., Bruno, G., Amiri Rudbari, H. & Khalaji, A.D. (2012). Synthesis, characterization and crystal structure determination of a new oxovanadium (IV) Schiff base complex: the catalytic activity in the epoxidation of cyclooctene. *Inorg. Chem. Commun.*, 18, 15–20.

11. Khalaji, A.D., Fejfarova, K. & Dusek, M. (2010). Synthesis and Characterization of Two Diimine Schiff Bases Derived from 2,4-Dimethoxybenzaldehyde: The Crystal Structure of N,N'-Bis(2,4 dimethoxybenzylidene)-1,2-diaminoethane. *Acta Chim. Slov.*, 57, 257–261.

12. Khalaji, A.D., Najafi Chermahini, A., Fejfarova, K. & Dusek, M. (2010). Synthesis, characterization, crystal structure, and theoretical studies on Schiff-base compound 6-[(5-Bromopyridin-2-yl) iminomethyl] phenol. *Struct. Chem.*, 21(1), 153–157.

13. Khandar, A.A. & Rezvani, Z. (1999). Preparation and thermal properties of the bis [5-((4-heptyloxyphenyl) azo)-N-(4-alkoxyphenyl)-salicylaldiminato] copper (II) complex homologues. *Polyhedron*, 18, 129.

14. El-Deen, I.M., Belal, A.A.M., Farid, N.Y., Zakaria, R. & Refat, M.S. (2015). Synthesis, spectroscopic, coordination and biological activities of some transition metal complexes containing ONO tridentate Schiff base ligand. *Spectrochimica Acta Part A*, 149, 771–787.

15. Bauer, A.W., Kirby, W.M.M., Sherris, J.C. & Turck, M. (1966). Antibiotic susceptibility testing by a standardized single disk method. *Am. J. Clin. Pathol.*, 36, 493–496.

16. Geary, W. (1971). The use of conductivity measurements in organic solvents for the characterisation of coordination compounds. *J. Coord. Chem. Rev.*, 7, 81–122.

17. Kavitha, P. & Reddy, K.L. (2016). Synthesis, spectral characterisation, morphology, biological activity and DNA cleavage studies of metal complexes with chromone Schiff base. *Arabian J. Chem.*, 9, 596–605.

18. Bellamy, L.J. (1980). *The Infrared Spectra of Complex Molecules*, Chapman and Hall, London.

19. Hanai, K. & Maki, Y. (1993). Vibrational spectra of β -lactams—III. potassium 2-azetidinone-1-sulfonate and its isotopic compounds. *Spectrochim Acta A*, 49, 1131–1137.

20. Wojciechowski, K. & Jerzy, S. (2000). Effect of the sulphonic group position on the properties of monoazo dyes. *Dyes and Pigments*, 44, 137–147.

21. Socrates, G. (1980). *Infrared Characteristic Group Frequencies*. John Wiley and Sons, New York.

22. Snehalatha, M., Ravikumar, C., Sekar, N., Jayakumar, V.S., & Joe, I.H. (2008). F.T-Raman, IR and UV-visible spectral investigations and *ab initio* computations of a nonlinear food dye amaranth. *J. Raman Spectrosc.*, 39, 928–936.

23. Socrates, G. (2001). *Infrared and Raman Characteristic Group Frequencies*. John Wiley and Sons, Chichester.

24. Lever, A.B.P. (1997). *Inorganic Electronic Spectroscopy*. 2nd ed., Elsevier, Amsterdam.

25. Wang, H., Zhao, P., Shao, D., Zhang, J. & Zhu, Y. (2009). Synthesis, characterization and spectra studies on Zn (II) and Cu (II) complexes with thiocarbamide ligand containing Schiff base group. *Struct. Chem.*, 20, 995–1003.

26. Raman, N., Ravichandran, S. & Thangarajan, C. (2004). Copper (II), cobalt (II), nickel (II) and zinc (II) complexes of Schiff base derived from benzil-2, 4-dinitrophenylhydrazone with aniline. *J. Chem. Sci.*, 116, 215–219.

27. Lever, A.B.P. (1968). Electronic spectra of some transition metal complexes: Derivation of Dq and B. *J. Chem. Edu.*, 45, 711.

28. Ramam, N., Kulandaisami, A. & Shunmugasundaram, A. (2001). Synthesis, spectral, redox and antimicrobial activities of Schiff base complexes derived from 1-phenyl-2, 3-dimethyl-4-aminopyrazol-5-one and acetoacetanilide. *Trans. Met. Chem.*, 26, 131135.

29. Sankhala, D.S., Mathur, R.C. & Mishra, S.N. (1980). Synthesis, magnetic and spectral studies on some adducts of manganese (II) acetylacetonate. *Indian J. Chem.*, 19A, 75–82.

30. Hathaway, B.J. & Billing, D.E. (1970). The electronic properties and stereochemistry of mono-nuclear complexes of the copper (II) ion. *Coord. Chem. Rev.*, 5, 143–207.

31. Hathaway, B.J. (1984). A new look at the stereochemistry and electronic properties of complexes of the copper (II) ion. *Struct. Bonding (Berlin)*, 57, 55.

32. Coats, A.W. & Redfern, J. P. (1964). Kinetic parameters from thermogravimetric data. *Nature*, 201, 68–69.

33. Horowitz, H.W. & Metzger, G.A. (1963). A new analysis of thermogravimetric traces. *Anal. Chem.*, 35, 1464–1468.

34. Chourasia, P., Suryesh, K.K. & Mishra, A.P. (1993). Synthesis and structural investigation of some mixed-ligand selenite complexes of cobalt (II). *Proc. Ind. Acad. Sci.*, 105, 173–181.

35. Frost, A.A. & Pearson, R.G. (1961). *Kinetics and Mechanism*, New York; Wiley.

36. Raman, N., Raja, S.J. & Sakthivel, A. (2009). Transition metal complexes with Schiff-base ligands: 4-aminoantipyrine based derivatives—a review. *J. Coord. Chem.*, 62, 691–709.

37. Kulkarni, A.D., Bagihalli, G.B., Patil, S.A. & Badami, P.S. (2009). Synthesis, characterization, electrochemical and *in-vitro* antimicrobial studies of Co(II), Ni(II), and Cu(II) complexes with Schiff bases of formyl coumarin derivatives. *J. Coord. Chem.*, 62, 3060–3072.

38. Li, F., Feterl, M., Mulayana, Y., Warner, J.M., Collins, J.G. & Keene, F.R. (2012). *In vitro* susceptibility and cellular uptake for a new class of antimicrobial agents: dinuclear ruthenium(II) complexes. *J. Antimicrob. Chemother.*, 67, 2686–2695.